Disentangling Intertwined Embedded-States and Spin Effects in Light-Front Quantization

Bernard L. G. Bakker[1] and Chueng-Ryong Ji[2]

[1] *Department of Physics and Astrophysics, Vrije Universiteit, De Boelelaan 1081, NL-1081 HV Amsterdam, Netherland*

[2] *Department of Physics, North Carolina State University, Raleigh, NC 27695-8202, USA*

Abstract

Despite the common belief, it is not always guaranteed that the light-front energy integration of the covariant Feynman amplitude automatically generates the equivalent amplitude in light-front quantization. Our example of a light-front calculation with a fermion loop explicitly shows that the persistent end-point singularity in the nonvalence contribution to the bad component of the current, J^-, leads to an infinitely different result from that obtained by the covariant Feynman calculation unless the divergence is properly subtracted. Ensuring the equivalence to the Feynman amplitude, we have identified the divergent term that needs to be removed from J^-. Only after this term is subtracted, the result is covariant and satisfies current conservation. The same calculation with the boson loop, however, doesn't exhibit such a singular behavior and without any adjustment yields the result identical to the Feynman amplitude. Numerical estimates of the nonvalence contributions are presented both for the cases of fermion and boson constituents.

I. INTRODUCTION

With the advent of Light-Front field theory, one can be quite hopeful to develop a connection between Quantum Chromodynamics (QCD) and the relativistic constituent quark model which is used in various electroweak form factor calculations. QCD provides a fundamental description of hadronic and nuclear structure in terms of elementary quark and gluon degrees of freedom. It is very succesful in the perturbative regime, for instance when it is used in the explanation of the evolution of distribution functions in deep-inelastic scattering. There, the basic hard interaction is described by perturbative QCD and the Electro-weak interaction. The soft parts, distribution and fragmentation functions, are non-perturbative ingredients, which are less well understood. Lattice calculations are becoming increasingly accurate, but there is still much room and need for other non-perturbative approaches.

It is part of the nature of the description of hadronic systems in terms of quarks and gluons that the characteristic momenta are of the same order or even very much larger than the masses of the particles involved. Therefore a relativistic treatment is called for. A very promising technique is Light-Front Dynamics (LFD), which treats relativistic many-body effects in a consistent way [1]. In LFD a Fock-space expansion of bound states is made. The wave function $\psi_n(x_i, k_i^\perp, \lambda_i)$ describes the component with n constituents, with longitudinal momentum fraction x_i, perpendicular momentum $k_i^\perp$ and helicity λ_i, $i = 1, \ldots, n$. It is the aim of LFD to determine those wave functions and use them in conjunction with hard scattering amplitudes to describe the properties of hadrons and their response to electroweak probes.

Recently, important steps were taken towards a realization of this goal. In the work of Brodsky,Hiller and McCartor [2], it is demonstrated how to solve the problem of renormalizing light-front Hamiltonian theories while maintaining Lorentz symmetry and other symmetries. (The genesis of the work presented in [2] may be found in [3] and additional examples including the use of LFD methods to solve the bound-state problems in field theory can be found in the review [1]). These results are indicative of the great potential of LFD for a fundamental description of non-perturbative effects in QCD. However, at present there are no realistic results available for wave functions of hadrons based on QCD alone. In order to calculate the response of hadrons to external probes, one might resort to the use of model wave functions. This way to estimate matrix elements was used by Ji et al. [4]. The same reasons that make LFD so attractive to solve bound-state problems in field theory make it also useful for a relativistic description of nuclear systems. Presently, it is realized that a parametrization of nuclear reactions in terms of non-relativistic wave functions must fail. LF methods have the advantage that they are formally similar to time-ordered many-body theories, yet provide relativistically invariant observables.

Until now we have sketched a rather rosy picture for the application of LFD to hadron physics. However, not all is well and this is just the reason for the present investigation. Since the 1980's it has been assumed that the observables computed in the framework of LFD using the methods of perturbation theory are invariants, just as in covariant perturbation theory. Many authors have shown that LFD has this feature in particular cases and some years ago some general statements to the same effect could be made [5,6]. A case in point is the calculation of a current matrix element in quantum field theory. A typical amplitude is given by the triangle diagram. One encounters this diagram e.g. when computing the pion

form factor (see Fig. 1).

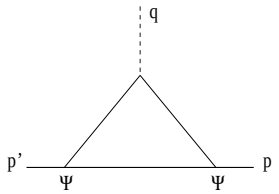

FIG. 1. Covariant triangle diagram

The vertices denoted by Ψ are coupling constants in covariant perturbation theory. The hard scattering process is the absorption of a photon of momentum q by a (anti-)quark. In the LFD approach the covariant amplitude is replaced by a series of LF time-ordered diagrams. In the case of the triangle diagram they are depicted in Fig. 2. The first of these

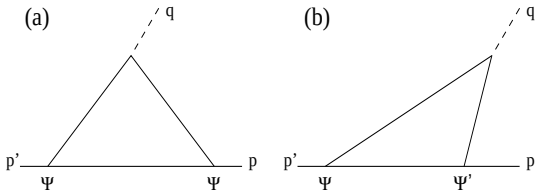

FIG. 2. Time-ordered triangle diagrams

two diagrams is easily interpreted in terms of the LF wave functions Ψ. However, the other diagram has a vertex that can again be written in the same way as before, but it contains also another vertex, denoted by Ψ', that cannot be written as a LF wave function. It is a new element in LFD. We call this vertex the *non-wave-function vertex*. In order to compute the form factors in the time-like region, the contributions from these vertices must be included. Semileptonic meson decay processes also require the contributions from these vertices. One may try to avoid using them by choosing special kinematic conditions. It is known however that this will not be a simple task [7,8].

In the present work, we investigate the contributions from the non-wave-function vertices. We construct both the wave-function and non-wave-function vertices using pointlike covariant ones. The model used here is essentially an extension of Mankiewicz and Sawicki's $(1+1)$-dimensional quantum field theory model [10], which was later reinvestigated by several others [6,11–14]. The starting model wave function is the solution of the covariant Bethe-Salpeter equation in the ladder approximation with a relativistic version of the contact interaction [11]. The covariant model wave function is a product of two free single particle propagators, the overall momentum-conserving Dirac delta function, and a constant vertex function. Consequently, all our form factor calculations are various ways of evaluating the Feynman triangle diagram in quantum field theory.

The importance of the contributions of the non-wave-function vertices was investigated in two cases: the electromagnetic form factors of a scalar and a pseudoscalar meson with spin-1/2 constituents. We also calculated the same form factor of a scalar meson with spin-0 constituents to see the spin effects. In 3+1 dimensions both the covariant and the LF

calculations are divergent and the model without any smeared vertex for the fermion loop is not well defined. This is in dramatic contrast to the case of spin-0 (boson) constituents, where regularization is not needed at all. In order to disentangle the issue of the non-wave-function vertices from the need of regularization, we performed our calculations in 1+1 dimensions, where at least the covariant calculations for spin-1/2 constituents give finite results.

It is commonly believed and widely used that the LF energy integration of the covariant Feynman amplitude generates the corresponding equivalent amplitude in the LFD. As we will show in this work, however, the equivalence between the LFD and the covariant Feynman calculation is not always guaranteed. The bad component of the current, J^-, with spin-1/2 constituents exhibits a persistent end-point singularity in the contribution from the non-wave-function vertex. Unless the divergence in this contribution is properly subtracted, the singular behavior leads to an infinitely different result from that obtained by the covariant Feynman calculation. Ensuring the equivalence to the Feynman amplitude, we have identified the divergent term that needs to be removed from J^-. Only after the identified term is subtracted, the result is covariant and satisfies the current conservation.

In the next Section (Section II), we present both the covariant Feynman calculations and the LF calculations using the LF energy integration for the electromagnetic form factors of a pseudoscalar and a scalar meson with spin-1/2 constituents as well as the same form factor of a scalar meson with spin-0 constituents. Section III contains the numerical estimates of both the wave-function and non-wave-function vertices to the electromagnetic form factors of each case presented in Section II. The conclusion and discussion follow in Section IV.

II. CALCULATIONS

The electromagnetic form factors can be extracted from the matrix elements of the current J^μ

$$\langle p'|J^\mu|p\rangle = ie_m(p'^\mu + p^\mu)F(q^2), \tag{2.1}$$

where e_m is the charge of the meson and $q^2 = (p'-p)^2$ is the square of the four momentum transfer. If one uses the plus-component, $J^+ = (J^0 + J^3)/\sqrt{2}$, the LF calculation gives two finite contributions, the wave-function part and the non-wave-function part, that add up to the covariant result, as expected. The importance of the non-wave-function contribution varies strongly with the momentum transfer and depends sensitively on the binding energy of the meson. For small values of q^2 and small binding energy, the wave-function part is dominant, but elsewhere the non-wave-function is essential for agreement between the LF calculation and the covariant results.

The form factor can also be extracted from the minus-component of the current, $J^- = (J^0 - J^3)/\sqrt{2}$. Covariance guarantees that it makes no difference whether the form factor is determined using the plus or the minus current matrix element. As LFD is not manifestly covariant, it may happen that J^- leads to a form factor different from the one determined using J^+. As we show in this Section, the matrix element of J^- diverges in LFD. Unless one regulates J^-, the current cannot be conserved. To assure the current conservation, it is crucial to identify the term that causes the divergence. We have identified this term exactly

and found that it is an infinite function of the momentum transfer. If this infinite term is subtracted, the two LF contributions become finite as it must be in the conserved current. Moreover, their sum equals again the covaraint result as expected. However, the regularized LF contributions are different from the two parts of the form factor extracted from the plus current. The differences grow with increasing binding energy.

A. Pseudoscalar Meson with the Fermion Loop

The covariant fermion triangle-loop (Fig. 1) for the pseudoscalar meson leads to the amplitude given by

$$\langle p'|J^\mu|p\rangle = 4N\int \frac{d^2k}{(2\pi)^2}\frac{(m^2-k^2+p\cdot p')k^\mu+(k^2-m^2-k\cdot p')p^\mu+(k^2-m^2-k\cdot p)p'^\mu}{(k^2-m^2+i\epsilon)((k-p)^2-m^2+i\epsilon)((k-p')^2-m^2+i\epsilon)}, \tag{2.2}$$

where m is the fermion mass and N modulo the obvious charge factor e_m is the normalization constant fixed by the unity of the form factor at zero momentum transfer. Even though we will present the unequal constituent mass case such as the kaon in the next Section of our numerical analysis, for the clarity of presentation we will focus in this Section on the equal mass case, such as the pion, only.

The usual Feynman parametrization and the covariant integration yields

$$\langle p'|J^\mu|p\rangle = i(p^\mu+p'^\mu)\frac{N}{\pi}\int_0^1 dx\int_0^{1-x} dy\frac{2m^2(1-x)-(m^2+(x+y-1)^2M^2-xyq^2)x}{((x+y)(x+y-1)M^2+m^2-xyq^2)^2}, \tag{2.3}$$

where M is the meson mass. For $q^2=0$, the integration leads to fix the normalization as

$$1/N = \frac{4m^2}{\pi M(4m^2-M^2)}\left[\frac{M}{4m^2}+\frac{1}{\sqrt{4m^2-M^2}}\arctan\left(\frac{M}{\sqrt{4m^2-M^2}}\right)\right]. \tag{2.4}$$

In LFD, the form factor $F(q^2)$ can be obtained by calculating either $\langle p'|J^+|p\rangle$ or $\langle p'|J^-|p\rangle$. In principle, the result must be identical to the above covariant Feynman result regardless of which component of the current is used. However, this is not necessarily the case as we demonstrate in the following.

First, the calculation of $\langle p'|J^+|p\rangle$ integrating out the LF energy k^- in Eq. (2.2) yields $F(q^2)$ given by

$$\begin{aligned} F(q^2) = \frac{N}{\pi(2+\alpha)}\Bigg[&\int_0^1 dx\frac{(1+\alpha)^2m^2}{[m^2-x(1-x)M^2][(1+\alpha)^2m^2-(1-x)(\alpha+x)M^2]} \\ &+\int_0^\alpha dx\frac{(1+\alpha)(\alpha-x)[x(\alpha-x)M^2-(1+\alpha)^2m^2]}{\alpha[(\alpha-x)(1+x)M^2-(1+\alpha)^2m^2][x(\alpha-x)M^2+(1+\alpha)m^2]}\Bigg], \end{aligned} \tag{2.5}$$

where α is given by $q^2=-\frac{\alpha^2M^2}{1+\alpha}$. In Eq. (2.5) the first and second terms correspond to the contributions from the wave-function and non-wave-function vertices depicted in the first and second diagrams in Fig. 2, respectively. We have verified that the contribution from the non-wave-function part vanishes at $\alpha=0$, *i.e.* at $q^2=0$, indicating the absence

of a zero-mode contribution [13] in the good component of the current J^+. Adding both contributions in Eq. (2.5), we obtain

$$F(q^2) = \frac{2N(1+\alpha)m^2}{\pi\alpha M[(2+\alpha)^2m^2-(1+\alpha)M^2]} \left[\frac{2+2\alpha+\alpha^2}{\sqrt{4(1+\alpha)m^2+\alpha^2M^2}}\text{Artanh}\left(\frac{\alpha M}{\sqrt{4(1+\alpha)m^2+\alpha^2M^2}}\right) + \frac{2\alpha}{\sqrt{4m^2-M^2}}\arctan\left(\frac{M}{\sqrt{4m^2-M^2}}\right)\right]. \quad (2.6)$$

This result is identical to the form factor obtained by the covariant Feynman calculation given by Eq. (2.3) and F(0)=1 gives the same normalization given in Eq. (2.4).

On the other hand, the calculation of $\langle p'|J^-|p\rangle$ yields $F(q^2)$ given by

$$F(q^2) = \frac{N}{\pi(2+\alpha)}\left[(1+\alpha)M^2\int_0^1 dx\frac{(1-x)^2}{[m^2-x(1-x)M^2][(1+\alpha)^2m^2-(1-x)(\alpha+x)M^2]} - \frac{(1+\alpha)^2m^2}{\alpha M^2}\int_0^\alpha\frac{dx}{\alpha-x}\frac{(1+\alpha)^2m^2+\{(1+\alpha)^2-(1+x)\}(\alpha-x)M^2}{[(\alpha-x)(1+x)M^2-(1+\alpha)^2m^2][x(\alpha-x)M^2+(1+\alpha)m^2]}\right], \quad (2.7)$$

where again it is apparent that the first and second terms correspond to the contributions from the wave-function and non-wave-function vertices, respectively. However, the non-wave-function part shows the end-point singularity coming from $\frac{1}{\alpha-x}$. Without subtracting the end-point singularity, the result is infinitely different from that obtained in the $\langle p'|J^+|p\rangle$ calculation. This is an astonishing result that deviates from the common belief in the equivalence of the LFD and the covariant Feynman calculation. Neither covariance nor current conservation is satisfied without a certain adjustment. In order to identify the term that must be subtracted, we rewrite the above equation as follows:

$$F(q^2) = \frac{N}{\pi(2+\alpha)}\left[(1+\alpha)M^2\int_0^1 dx\frac{(1-x)^2}{[m^2-x(1-x)M^2][(1+\alpha)^2m^2-(1-x)(\alpha+x)M^2]} + \int_0^\alpha dx\frac{R(x,\alpha)}{\alpha-x}\right], \quad (2.8)$$

where $R(x,\alpha)$ is defined by

$$R(x,\alpha) = -\frac{(1+\alpha)^2m^2[(1+\alpha)^2m^2+\{(1+\alpha)^2-(1+x)\}(\alpha-x)M^2}{\alpha M^2[(\alpha-x)(1+x)M^2-(1+\alpha)^2m^2][x(\alpha-x)M^2+(1+\alpha)m^2]}. \quad (2.9)$$

In order to obtain the identical result to Eq. (2.6) from the $\langle p'|J^+|p\rangle$ calculation, we find that $R(\alpha,\alpha)$ must be subtracted from the numerator of the non-wave-function part integrand, *i.e.*,

$$F(q^2) = \frac{N}{\pi(2+\alpha)}\left[(1+\alpha)M^2\int_0^1 dx\frac{(1-x)^2}{[m^2-x(1-x)M^2][(1+\alpha)^2m^2-(1-x)(\alpha+x)M^2]} + \int_0^\alpha dx\frac{R(x,\alpha)-R(\alpha,\alpha)}{\alpha-x}\right]. \quad (2.10)$$

The subtracted term $R(\alpha,\alpha)=\frac{1+\alpha}{\alpha M^2}$ depends on the momentum transfer and never vanishes. While the subtracted result Eq. (2.10) is identical to Eq. (2.6), it is interesting to note that the zero-mode contribution does not vanish in the $\langle p'|J^-|p\rangle$ calculation as the non-wave-function part in Eq. (2.10) still survives even at $q^2=0$. However, the subtracted result Eq. (2.10) with the zero-mode contribution assures covariance and satisfies current conservation.

B. Scalar Meson with the Fermion Loop

The Feynman parametrization and the covariant integration of the fermion triangle-loop for the scalar meson gives the following amplitude:

$$\begin{aligned}\langle p'|J^\mu|p\rangle &= 4N\int\frac{d^2k}{(2\pi)^2}\frac{(3m^2+k^2-p\cdot p')k^\mu-(k^2+m^2-k\cdot p')p^\mu-(k^2+m^2-k\cdot p)p'^\mu}{(k^2-m^2+i\epsilon)((k-p)^2-m^2+i\epsilon)((k-p')^2-m^2+i\epsilon)}\\ &= i(p^\mu+p'^\mu)\frac{N}{\pi}\int_0^1 dx\int_0^{1-x}dy\frac{x((1-x-y)^2M^2-m^2-xyq^2)}{((x+y)(x+y-1)M^2+m^2-xyq^2)^2},\end{aligned}\tag{2.11}$$

where the normalization N is again fixed by $F(0)=1$ and given by

$$1/N=\frac{4m^2}{\pi M^3}\left[\frac{M}{4m^2}-\frac{1}{\sqrt{4m^2-M^2}}\arctan\left(\frac{M}{\sqrt{4m^2-M^2}}\right)\right].\tag{2.12}$$

In LFD, the calculation of $\langle p'|J^+|p\rangle$ leads to $F(q^2)$ given by

$$\begin{aligned}F(q^2)=\frac{N}{\pi(2+\alpha)}\Bigg[&\int_0^1 dx\frac{(1+\alpha)\{2(1-x)(2x+\alpha)-(1+\alpha)\}m^2}{[m^2-x(1-x)M^2][(1+\alpha)^2m^2-(1-x)(\alpha+x)M^2]}\\ &+\int_0^\alpha dx\frac{(1+\alpha)(\alpha-x)[(1+\alpha)(1+4x-\alpha)m^2-x(\alpha-x)M^2]}{\alpha[(\alpha-x)(1+x)M^2-(1+\alpha)^2m^2][x(\alpha-x)M^2+(1+\alpha)m^2]}\Bigg],\end{aligned}\tag{2.13}$$

where the contribution from the non-wave-function part again vanishes at $q^2=0$, indicating the absence of zero-mode contribution [13] in the good component of the current, J^+. Adding both contributions, we find

$$\begin{aligned}F(q^2)=&\frac{2N(1+\alpha)m^2}{\pi\alpha M^3[(2+\alpha)^2m^2-(1+\alpha)M^2]}\\ &\Bigg[\frac{8(1+\alpha)m^2-(2+2\alpha-\alpha^2)M^2}{\sqrt{4(1+\alpha)m^2+\alpha^2M^2}}\mathrm{Artanh}\left(\frac{\alpha M}{\sqrt{4(1+\alpha)m^2+\alpha^2M^2}}\right)\\ &-\frac{2\alpha}{\sqrt{4m^2-M^2}}\arctan\left(\frac{M}{\sqrt{4m^2-M^2}}\right)\Bigg].\end{aligned}\tag{2.14}$$

This result is identical to the form factor obtained by the covariant Feynman calculation given by Eq. (2.11) and F(0)=1 gives the same normalization presented in Eq. (2.11).

However, the calculation of $\langle p'|J^-|p\rangle$ generates an end-point point singularity similar to the one observed in the pseudoscalar case. Defining the function

$$S(x,\alpha)=\frac{(1+\alpha)^2m^2[(1+\alpha)(1+4x-3\alpha)m^2+\{\alpha(2-\alpha)+(2\alpha-1)x\}(\alpha-x)M^2]}{\alpha M^2[(\alpha-x)(1+x)M^2-(1+\alpha)^2m^2][x(\alpha-x)M^2+(1+\alpha)m^2]}, \tag{2.15}$$

we find $F(q^2)$ given by

$$F(q^2)=\frac{N}{\pi(2+\alpha)}\Bigg[-\frac{(1+\alpha)}{M^2}\int_0^1 dx\frac{4(1+\alpha)m^4-2(2+\alpha)(1-x)m^2M^2+(1-x)^2M^4}{[m^2-x(1-x)M^2][(1+\alpha)^2m^2-(1-x)(\alpha+x)M^2]} + \int_0^\alpha dx\frac{S(x,\alpha)}{\alpha-x}\Bigg], \tag{2.16}$$

where the non-wave-function part again shows the end-point singularity coming from $\frac{1}{\alpha-x}$. In order to obtain the identical result to Eq. (2.14) from the $\langle p'|J^+|p\rangle$ calculation, we find that $S(\alpha,\alpha)$ must be subtracted from the numerator of the non-wave-function part integrand, *i.e.*,

$$F(q^2)=\frac{N}{\pi(2+\alpha)}\Bigg[-\frac{(1+\alpha)}{M^2}\int_0^1 dx\frac{4(1+\alpha)m^4-2(2+\alpha)(1-x)m^2M^2+(1-x)^2M^4}{[m^2-x(1-x)M^2][(1+\alpha)^2m^2-(1-x)(\alpha+x)M^2]} + \int_0^\alpha dx\frac{S(x,\alpha)-S(\alpha,\alpha)}{\alpha-x}\Bigg]. \tag{2.17}$$

The subtracted term $S(\alpha,\alpha)=-\frac{1+\alpha}{\alpha M^2}$ again cannot vanish. The zero-mode contribution is also visible since the second term in Eq. (2.17) doesn't vanish even if $q^2=0$. The subtracted result Eq. (2.17), however, assures the covariance and satisfies the current conservation as in the previous calculation of the pseudoscalar meson.

C. Scalar Meson with the Boson Loop

For a comparison with the scalar constituents neglecting spin effects, we present in this subsection the calculation of $F(q^2)$ for a scalar meson with a boson loop. The Feynman parametrization and the covariant integration of the boson triangle-loop for the scalar meson gives the following amplitude:

$$\begin{aligned}\langle p'|J^\mu|p\rangle &= N\int\frac{d^2k}{(2\pi)^2}\frac{p^\mu+p'^\mu-2k^\mu}{(k^2-m^2+i\epsilon)((k-p)^2-m^2+i\epsilon)((k-p')^2-m^2+i\epsilon)}\\ &= i(p^\mu+p'^\mu)\frac{N}{4\pi}\int_0^1 dx\int_0^{1-x}dy\frac{2x-1}{((x+y)(x+y-1)M^2+m^2-xyq^2)^2},\end{aligned} \tag{2.18}$$

where the normalization N is given by

$$1/N=\frac{1}{2\pi M^2(4m^2-M^2)}\left[-1+\frac{2(2m^2-M^2)}{M\sqrt{4m^2-M^2}}\arctan\left(\frac{M}{\sqrt{4m^2-M^2}}\right)\right]. \tag{2.19}$$

In LFD, the calculation of $\langle p'|J^+|p\rangle$ leads to $F(q^2)$ given by

$$F(q^2) = \frac{N}{4\pi(2+\alpha)}\Bigg[-1\int_0^1 dx \frac{(1+\alpha)(2x+\alpha)(1-x)}{[m^2-x(1-x)M^2][(1+\alpha)^2m^2-(1-x)(\alpha+x)M^2]} + \int_0^\alpha dx \frac{(1+\alpha)^2(\alpha-2x)(\alpha-x)}{\alpha[(\alpha-x)(1+x)M^2-(1+\alpha)^2m^2][x(\alpha-x)M^2+(1+\alpha)m^2]}\Bigg], \quad (2.20)$$

where the contribution from the non-wave-function part again vanishes at $q^2 = 0$, indicating the absence of a zero-mode contribution [13] in the good component of the current J^+ as in the fermion loop cases. Adding both contributions, we find

$$F(q^2) = \frac{N(1+\alpha)}{2\pi\alpha M^3[(2+\alpha)^2m^2-(1+\alpha)M^2]} \Bigg[-\sqrt{4(1+\alpha)m^2+\alpha^2M^2}\,\mathrm{Artanh}\left(\frac{\alpha M}{\sqrt{4(1+\alpha)m^2+\alpha^2M^2}}\right) + \frac{2\alpha(2m^2-M^2)}{\sqrt{4m^2-M^2}}\arctan\left(\frac{M}{\sqrt{4m^2-M^2}}\right)\Bigg]. \quad (2.21)$$

This result is identical to the form factor obtained by the covariant Feynman calculation given by Eq. (2.18) and F(0)=1 gives the same normalization presented in Eq. (2.19).

Similarly, the calculation of $\langle p'|J^-|p\rangle$ generates $F(q^2)$ given by

$$F(q^2) = \frac{N}{4\pi(2+\alpha)}\Bigg[\frac{(1+\alpha)}{M^2}\int_0^1 dx \frac{2(1+\alpha)m^2-(2+\alpha)(1-x)M^2}{[m^2-x(1-x)M^2][(1+\alpha)^2m^2-(1-x)(\alpha+x)M^2]} + \frac{(1+\alpha)^2}{\alpha M^2}\int_0^\alpha dx \frac{2(1+\alpha)m^2+\alpha(\alpha-x)M^2}{[(\alpha-x)(1+x)M^2-(1+\alpha)^2m^2][x(\alpha-x)M^2+(1+\alpha)m^2]}\Bigg]. \quad (2.22)$$

Unlike the cases of fermion constituents, however, the non-wave-function part here does not exhibit the end-point singularity. Without any adjustment, we find that Eq. (2.22) is identical to Eq. (2.21) obtained from $\langle p'|J^+|p\rangle$. Thus, the result is automatically covariant and satisfies current conservation. However, the zero-mode contribution is still present in J^- current as one can easily see that the second term in Eq. (2.22) doesn't vanish when α goes to zero. In the next section, we numerically estimate the importance of the non-wave-function part in all three cases that we presented in this section.

III. NUMERICAL RESULTS

We have estimated both the wave-function and non-wave-function vertices to the electromagnetic form factors of each case presented in Section II. For the three cases (A,B,C) presented in Section II, we show the numerical results of the form factor calculated via the minus component as well as the plus component of the current. We denote the contributions from the wave-function and non-wave-function vertices as $F_{\rm val}^{+(-)}$ and $F_{\rm nv}^{+(-)}$, respectively when the plus(minus) component of the current is used. The sum of the two contributions is denoted by $F_{\rm tot}^{+(-)}$,*i.e.* $F_{\rm tot}^{+(-)} = F_{\rm val}^{+(-)} + F_{\rm nv}^{+(-)}$.

For the numerical computation, we take for the experimental meson masses of the pion and the kaon $m_\pi = 0.140$ GeV and $m_K = 0.494$ GeV resp. and vary the quark masses to investigate the binding-energy dependence of the meson form factors. We call the pseudoscalar

meson with the equal quark masses and mass $m_\pi = 0.140$ GeV the "pion". Likewise, the pseudoscalar meson with the unequal quark masses and the meson mass $m_K = 0.494$ GeV is called the "kaon".

The "pion" form factor with the quark mass $m_q = 0.250$ GeV is shown in Fig. 3. When the plus current is used, the valence contribution $F^+_{\rm val}$ diminishes very quickly as Q^2 gets larger even though the normalization at $Q^2 = 0$ is entirely coming from the valence part as we pointed out in Section II. The crossing between $F^+_{\rm val}$ and $F^+_{\rm nv}$ appears at Q^2 below 0.05 GeV^2. When the minus current is used, however, the valence contribution $F^-_{\rm val}$ is negligible even at $Q^2 = 0$ and the entire result is essentially given by $F^-_{\rm nv}$. The value of $F^-_{\rm nv}(0)$ corresponds to the zero-mode contribution in the minus current J^- and it is interesting to note that more than 90% of the form factor at $Q^2 = 0$ is contributed by the zero-mode. Since $F^+_{\rm tot} = F^-_{\rm tot}$ exactly coincide with the covariant result obtained by Eq.(3) for all Q^2 as they must, only a single solid line is depicted in Fig. 3. The same applies to all of the other figures presented in this work.

In Fig. 4, we present the results for the "pion" by changing the quark masses in the following way: $m_q = 0.140$, 0.077 and 0.0707 GeV, respectively. The closer m_q is to $m_\pi/2 = 0.07$ GeV, the smaller the binding energy gets, and the slope of $F^{+/-}_{\rm tot}$ at $Q^2 = 0$ (or the charge radius) increases with decreasing quark mass, as expected. We find that the crossing between $F^+_{\rm val}$ and $F^+_{\rm nv}$ occurs at a larger value of Q^2 and $F^-_{\rm val}$ becomes larger near $Q^2 = 0$ as the binding gets weaker. This may be explained by the reduction of the probability to generate the non-wave-function vertex (or the higher Fock state) compared to the valence state as the interaction between the constituents gets weaker. Thus, in the weaker binding, $F^+_{\rm val}$ dominates over $F^+_{\rm nv}$. Similarly, $F^-_{\rm val}$ becomes the main contribution near $Q^2 = 0$ which is the only region where the form factor exists in the weak binding limit. Consequently, the zero-mode $F^-_{\rm nv}(0)$ gets substantially diminished as shown in Fig. 4.

The "kaon" form factor with $m_q = 0.25$ GeV and $m_s = 0.37$ GeV is shown in Fig. 5. Compared to the "pion" case, the dominance of $F^+_{\rm val}$ extends to the larger Q^2 region and the crossover between $F^+_{\rm val}$ and $F^+_{\rm nv}$ is postponed beyond the range of $Q^2 = 1$ GeV^2. The zero-mode $F^-_{\rm nv}(0)$ is also much smaller than in the "pion" case even though $F^-_{\rm nv}$ rises very quickly as Q^2 gets away from the zero range. As one can see in Figs.5(a) and (b), the contribution from the heavier quark struck by the photon is larger than that from the lighter quark struck by the photon. We have indeed confirmed that as m_s gets larger only the contribution from the heavy quark struck by the photon dominates as expected.

In Fig. 6, the form factors of the scalar partner to the "pion", which we call "s-pion" in the following, with $m_q = 0.25$, 0.14, 0.077, and 0.0707 GeV are presented for comparison with the "pion" case. The basic features of $F^+_{\rm val}$ and $F^+_{\rm nv}$ near $Q^2 = 0$ are same as in the "pion" case because $F^+_{\rm val}(0) = 1$ must hold for any meson. However, as the binding gets weaker, we find that the "s-pion" form factors $F^{+/-}_{\rm tot}$ change sign at smaller Q^2-values. This indicates that electron scattering off the "s-pion" not only has zero cross section at a certain electron energy, but also that the electron energy that yields zero scattering gets smaller as the binding of the "s-pion" is weaker. Another dramatic difference from the pseudoscalar meson is the astonishing cancellation between $F^-_{\rm val}$ and $F^-_{\rm nv}$. Especially in the strong binding case, both $F^-_{\rm val}$ and $F^-_{\rm nv}$ are huge but they cancel in a very remarkable way to yield exactly the same result as $F^+_{\rm tot}$.

In Fig. 7, the form factor of the scalar partner to the "kaon", *i.e.* "s-kaon", is plotted.

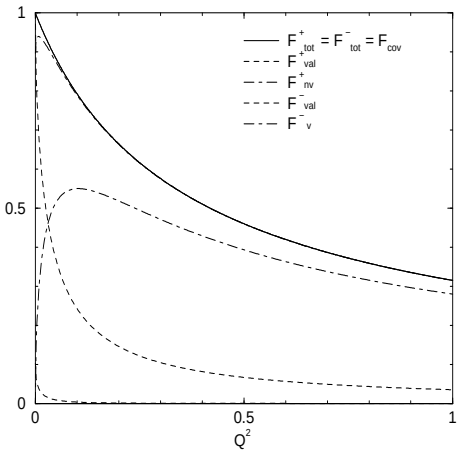

FIG. 3. Pion form factor in LF calculation in 1+1 Dim. Pseudoscalar meson with spinor consitutents. $M = 0.140$ GeV, $m_q = 0.250$ GeV. Fat lines correspond to the plus-current, thin lines to the minus-current. The solid line is the full form factor. It is the sum of the valence and the non-valence contributions. The separate contributions differ but the sums coincide. The form factor determined from the covariant amplitude is identical with the full form factor determined in the LF calculation.

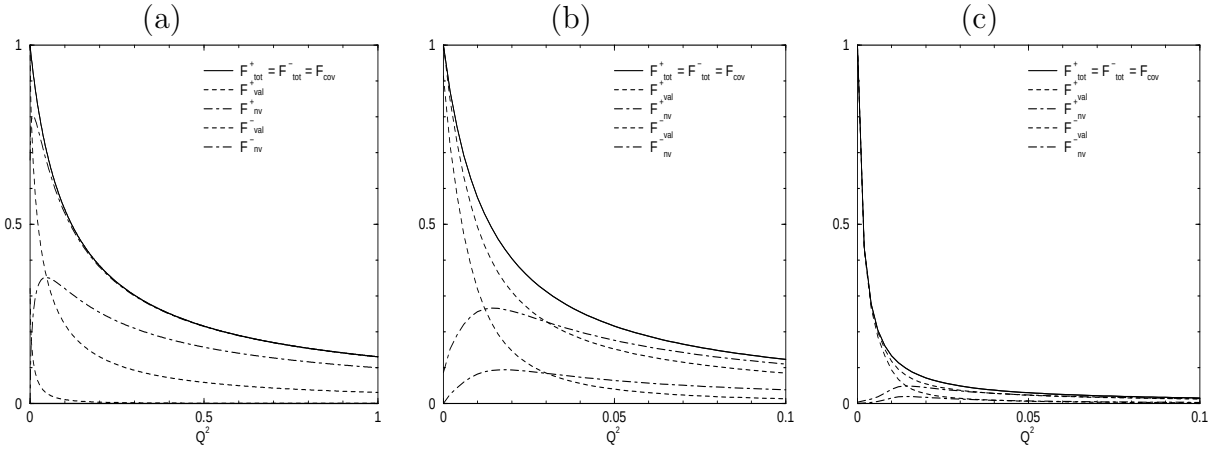

FIG. 4. "Pion" form factor in LF calculation in 1+1 Dim. Pseusoscalar meson with spinor consitutents. (a) $m_\pi = 0.140$, $m_q = 0.140$. (b) $m_\pi = 0.140$, $m_q = 0.077$. (c) $m_\pi = 0.140$, $m_q = 0.0707$. The lines have the same meaning as in Fig. 3. Note the change in scale in panels (b) and (c).

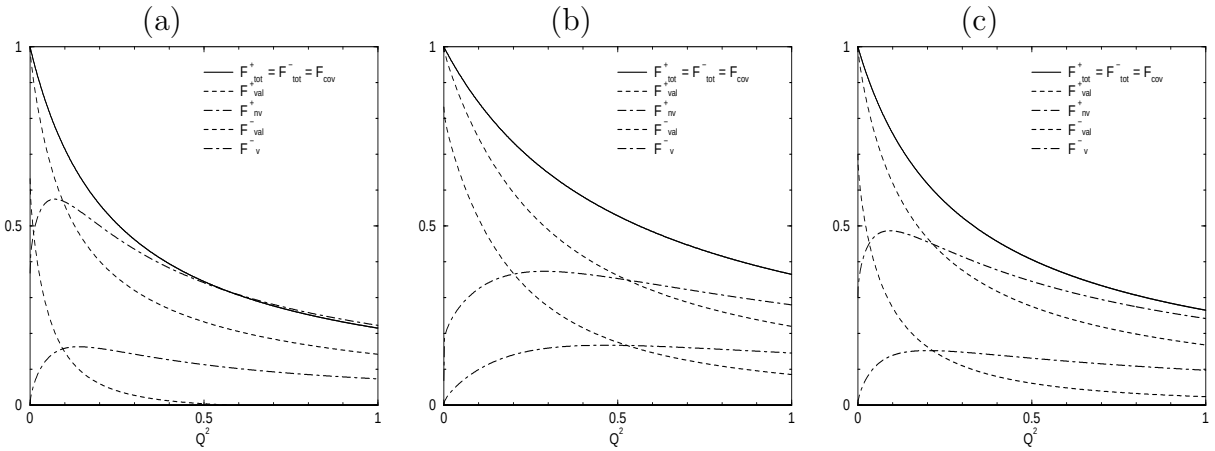

FIG. 5. Kaon form factor. LFD calculation in 1+1 Dim. $m_K = 0.494$, $m_q = 0.250$, $m_s = 0.370$. (a) Charge +1 on the light quark, (b) charge +1 on the strange quark, (c) $e_q = 2/3$, $e_s = 1/2$. The lines have the same meaning as in Fig. 3.

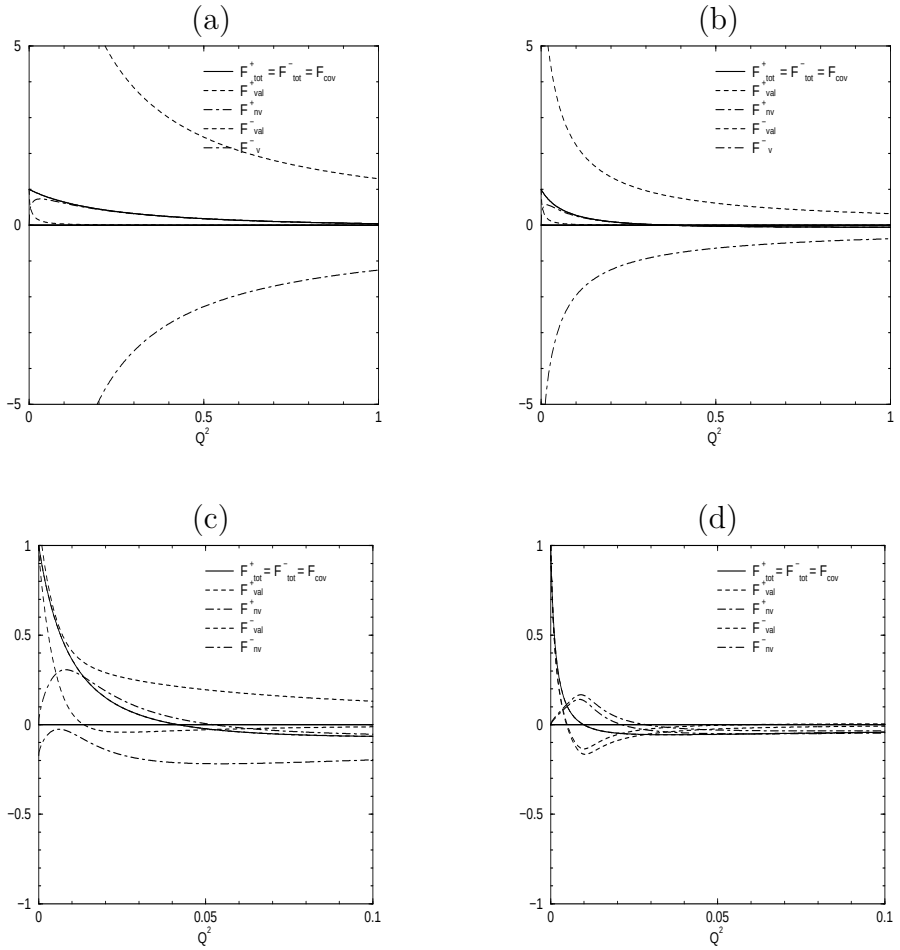

FIG. 6. "Pion" form factor in LF calculation in 1+1 Dim. Scalar meson with spinor constituents. (a) $m_\pi = 0.140$, $m_q = 0.250$. (b) $m_\pi = 0.140$, $m_q = 0.140$. (c) $m_\pi = 0.140$, $m_q = 0.077$. (d) $m_\pi = 0.140$, $m_q = 0.0707$. Note the change in scales in the latter two panels. The lines have the same meaning as in Fig. 3.

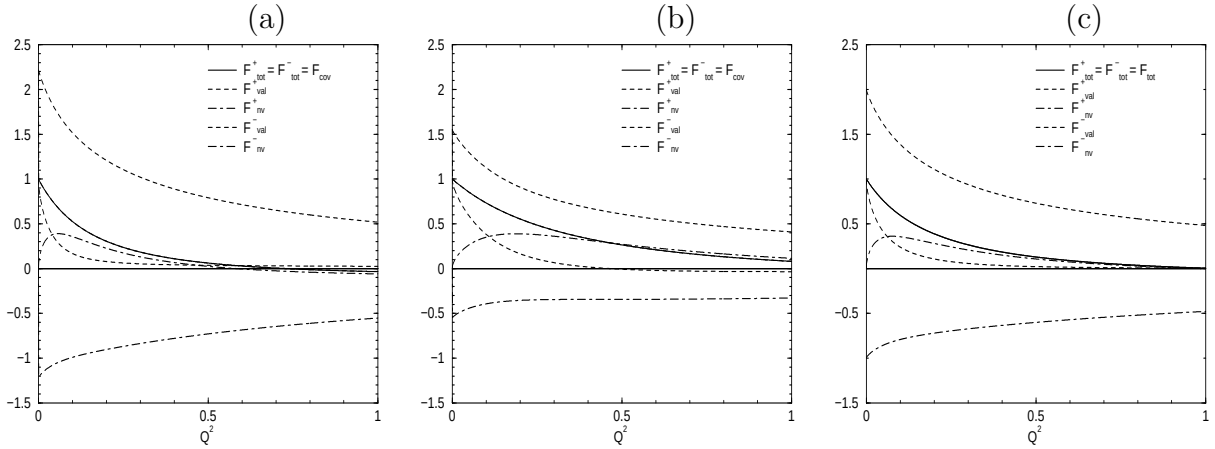

FIG. 7. "S-Kaon" form factor LFD calculation in 1+1 Dim. Spinor quarks. $m_K = 0.494$, $m_q = 0.250$, $m_s = 0,370$. (a) Charge +1 on the light quark, (b) charge +1 on the heavy quark, (c) $e_q = 2/3$, $e_s = 1/2$. The lines have the same meaning as in Fig. 3.

The basic feature is similar to the "s-pion". In Fig. 8, we show the results for the "s-pion" when the spinor quark is replaced by a bosonic quark. As we extensively discussed in Section II, the subtraction of the end-point singularity is not required in the scalar quark case in contrast to the spinor quark case. In the scalar quark case, it is interesting to note that $F^-_{\rm val}$ and $F^-_{\rm nv}$ reveal a large difference compare to the spinor quark case, while $F^+_{\rm val}$ and $F^+_{\rm nv}$ are very similar to the spinor quark case. We find that the huge cancellation between $F^-_{\rm val}$ and $F^-_{\rm nv}$ observed in the spinor quark case does occur in the scalar quark case only for very strong binding, and the most of $F^-_{\rm tot}$ is saturated by $F^-_{\rm nv}$. However, the tiny contribution from $F^-_{\rm val}$ near $Q^2 = 0$ grows as the binding gets weaker and we have demonstrated the dominance of the valence part in the small binding limit regardless of the spin content, as discussed above. Fig. 9 shows the corresponding results for the "s-kaon" when the spinor quark is replaced by a bosonic quark. While the general features are similar to the spinor quark case, the bosonic quarks are more tightly bound together than the spinor quarks so that the charge radius of the meson is smaller than the case of spinor quarks as one might expect from the Pauli's exclusion principle.

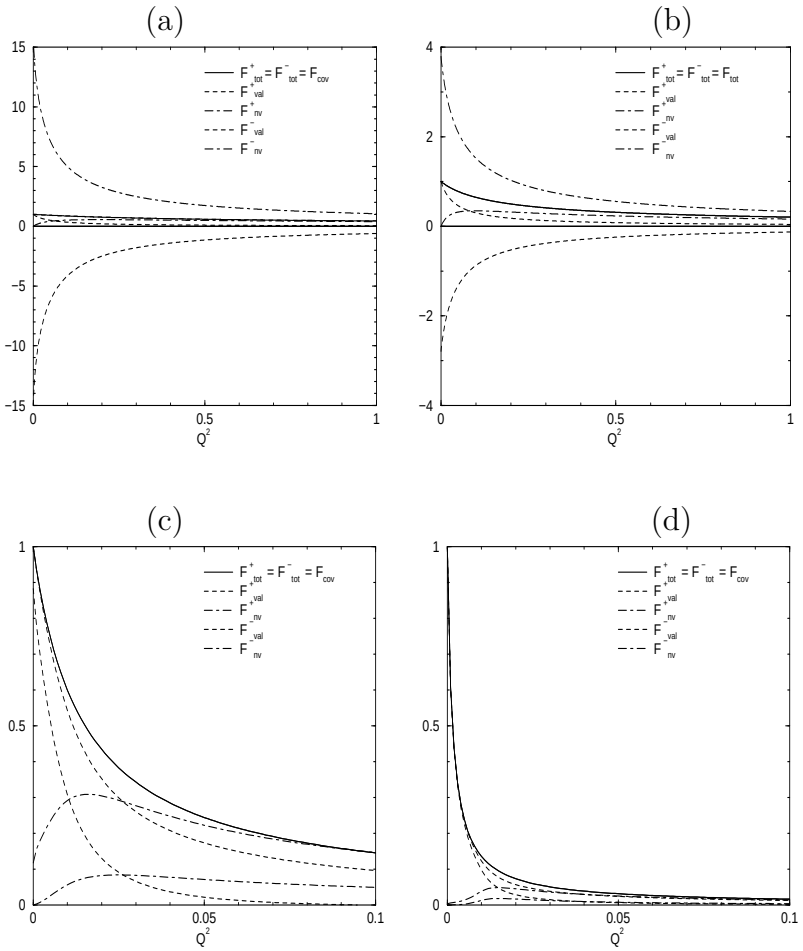

FIG. 8. "Pion" form factor in LF calculation in 1+1 Dim. Scalar meson with boson constituents. (a) $m_\pi = 0.140$, $m_q = 0.250$. (b) $m_\pi = 0.140$, $m_q = 0.140$. (c) $m_\pi = 0.140$, $m_q = 0.077$. (d) $m_\pi = 0.140$, $m_q = 0.0707$. Note the change in scales in the latter two panels. The lines have the same meaning as in Fig. 3.

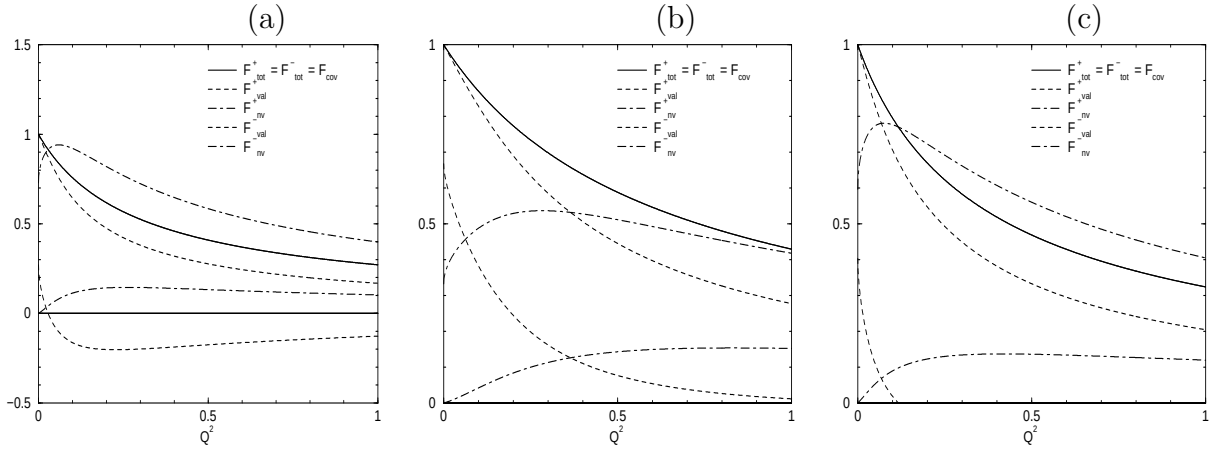

FIG. 9. "S-kaon" form factor LFD calculation in 1+1 Dim. Boson quarks $m_K = 0.494$, $m_q = 0.250$, $m_s = 0,370$. (a) Charge +1 on the light quark, (b) charge +1 on the heavy quark, (c) $e_q = 2/3$, $e_s = 1/2$. The lines have the same meaning as in Fig. 3.

IV. CONCLUSION AND DISCUSSION

In this paper, we have analyzed both the plus and minus components of the current quantized on the light-front to compute the electromagnetic form factors of pseudoscalar and scalar mesons. We considered spin-1/2 consituents as well as spin-0 constituents and found dramatic differences between the two cases. Comparing with the covariant Feynman calculations, we notice that the common belief of equivalence between the manifestly covariant calculation and the LF calculation linked by the LF energy integration of the Feynman amplitude is not always realized. The minus component of the LF current generated by the fermion loop has a persistent end-point singularity that must be removed to assure covariance and current conservation. A similar singularity was observed in the calculation of the fermion self-energy in [6] and [3]. The plus component of the LF current, however, is immune to this disorder and provides a form factor identical to the one obtained doing the covariant Feynman calculation. This phenomenon is also associated with the spin-effect of the constituents because the calculation with the scalar(spin-0) constituents does not have the same symptom. Decomposing the LF amplitude into the wave-function and non-wave-function parts, it is interesting to note that the end-point singularity exists only in the non-wave-function vertex contribution.

Even after the singularity is removed, the minus component of the current sustains the zero-mode contribution while the plus component is free from the zero-mode. We have numerically estimated the importance of the non-wave-function vertices in all three cases that we discussed in Section II. We considered also the unequal constituent mass cases such as the kaon form factor. We find that the behaviors of F^-_{val} and F^-_{nv} are trimendously different between pseudoscalar and scalar meson cases, while F^+_{val} and F^+_{nv} have very similar features in both cases. The huge but remarkably exact cancellation between F^-_{val} and F^-_{nv} shown in the scalar meson case persists even if the spinor quark is replaced by the bosonic quark. In the bosonic quark case, however, the binding between the constituents is stronger than the spinor quark case. We also notice that the zero-mode $F^-_{nv}(0)$ diminishes as the binding gets weaker. Our results are quite consistent to the earlier observation [13] exhibiting the smaller zero-mode contribution in the heavier quark systems. In all of these cases, our results show that if the meson is weakly bound then the contributions from the wave-function and the non-wave-function vertices to the plus current are separately almost the same as those for the minus current. Of course, their sums add up to the same number as the covariant Feynman result in both the plus and minus cases.

The calculations carried out so far are semi-realistic as the model was 1+1-dimensional and only a point-vertex was considered. It is clear from a formal analysis of the 3+1-dimensional case, however, that a singularity of the same form will occur in the matrix element of J^- calculated in LFD regardless of dimensionality. A recent analysis of the Burkhardt-Cottingham sum-rule seems to reveal a similar divergence in the polarized spin-1/2 structure functions [15]. While the additional regularization may be provided by smearing the point-vertex with a realistic wave-function in the 3+1-dimensional covariant treatment of the current, the identification of the singular term as we achieved in this work would still be necessary for the smeared vertex cases. The importance of the non-wave-function parts may nevertheless differ numerically from the 1+1-dimensional case. This point is presently under investigation.

ACKNOWLEDGMENTS

This work was supported in part by a grant from the US Department of Energy and the Netherlands Organisation for Scientific Research (NWO).

REFERENCES

[1] S.J. Brodsky, H.C. Pauli, and S.S. Pinsky, *Quantum Chromodynamics and Other Field Theories on the Light Cone*, Phys. Rept. **301**, 299 (1998).

[2] S.J. Brodsky, J.R. Hiller, and G. McCartor, Phys. Rev. **D58**, 025005 (1998);
J.R. Hiller, *Pauli-Villars Regularization in a Discrete Light Cone Model*, hep-ph/9807245.

[3] D.G.Robertson and G.McCartor, Z. Phys. **C53**, 661 (1992); G.McCartor and D.G.Robertson, Z.Phys. **C53**, 679 (1992).

[4] C.R. Ji, Acta Phys. Polon. **B27**, 3377-3380 (1996);
H.M. Choi and C.R. Ji, Phys. Rev. **D59**, 034001 (1999); Phys. Rev. **D59**, 074015 (1999); Phys. Lett. **B460**, 461 (1999)

[5] N.E. Ligterink and B.L.G. Bakker, Phys. Rev. **D52**, 5954 (1995);
N.E. Ligterink and B.L.G. Bakker, Phys. Rev. **D52**, 5917 (1995).

[6] N.C.J. Schoonderwoerd and B.L.G. Bakker, Phys. Rev. **D57**, 4965 (1998);
N.C.J. Schoonderwoerd and B.L.G. Bakker, Phys. Rev. **D58**, 0250013 (1998).

[7] J.P.B.C. de Melo, J.H.O.de Sales, T. Frederico, and P.U. Sauer, Nucl. Phys, **A631**, 574 (1998);
J.P.B.C. de Melo, H.W.L. Naus, and T. Frederico, *Pion Electromagnetic Current in the Ligth-Cone Formalism*, hep-ph/971022.

[8] W. Jaus, Phys. Rev. **D60**, 054026 (1999).

[9] N.B. Demchuk, I.L. Grach, I. M.Narodetskii, and S. Simula, Phys. At. Nuclei **59**, 2152 (1996);
I.L. Grach, I.M. Narodetskii, and S. Simula, Phys. Lett. **B385**, 317 (1996);
S. Simula, Phys. Lett. **B373**, 193 (1996);
H.-Y. Cheng, C.-Y. Cheng and C.-W. Hwang, Phys. Rev. **D55**, 1559 (1997).

[10] M. Sawicki and L. Mankiewicz, Phys. Rev. D **37**, 421 (1988);
L. Mankiewicz and M. Sawicki, *ibid.* **40**, 3415 (1989).

[11] S. Głazek and M. Sawicki, Phys. Rev. D **41**, 2563 (1990).

[12] M. Sawicki, Phys. Rev. D **44**, 433 (1991); *ibid.* **46**, 474 (1992).

[13] H.-M. Choi and C.-R. Ji, Phys. Rev. D **58**, 071901 (1998).

[14] S. J. Brodsky and D. S. Hwang, Nucl. Phys. B **543**, 239 (1998).

[15] M. Burkardt, talk presented at the Stanfest, University of Georgia, 1999.

Cov SB

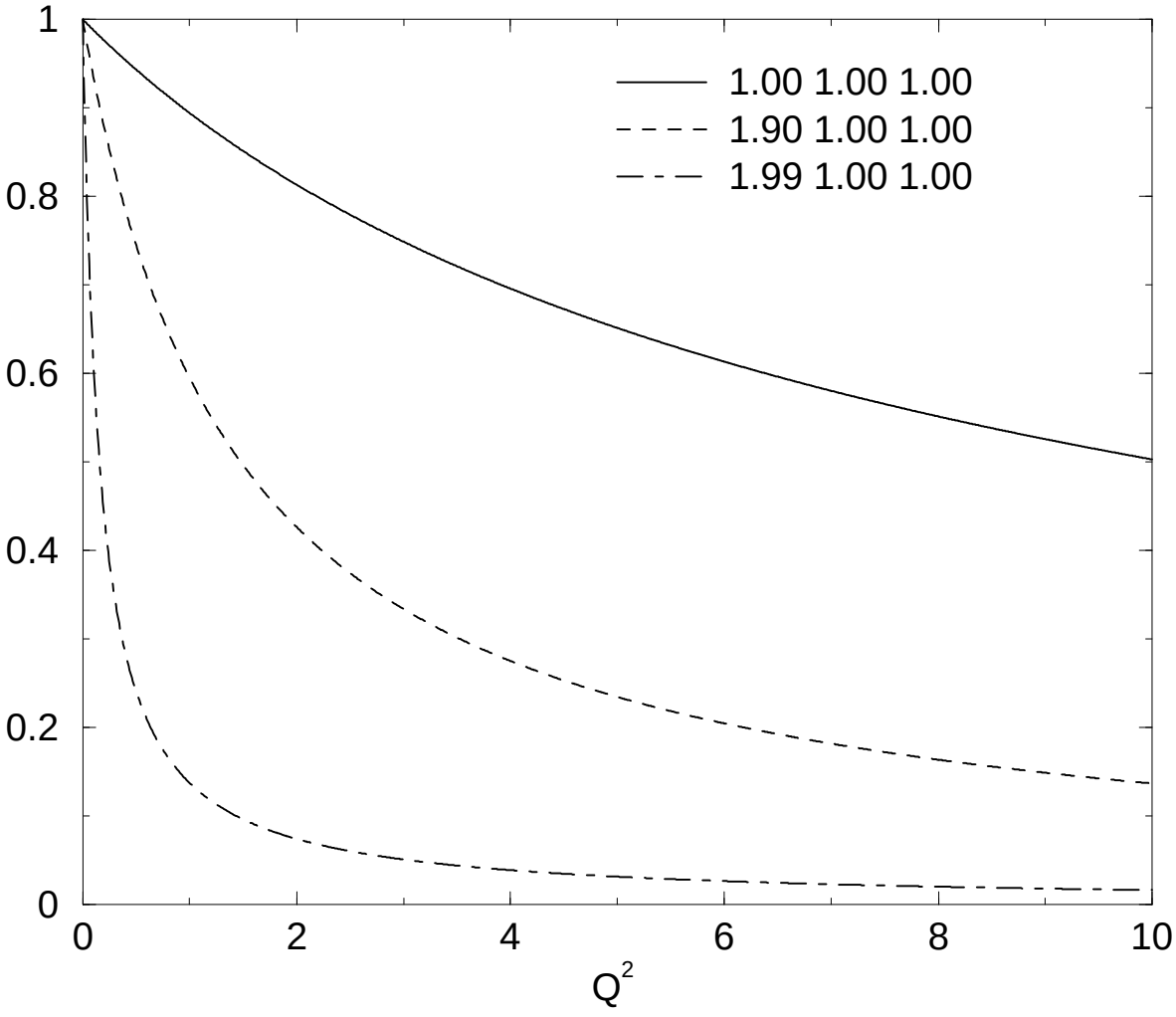

Scalar Pion, Spinor Quarks

M=0.140 m_q=0.0707

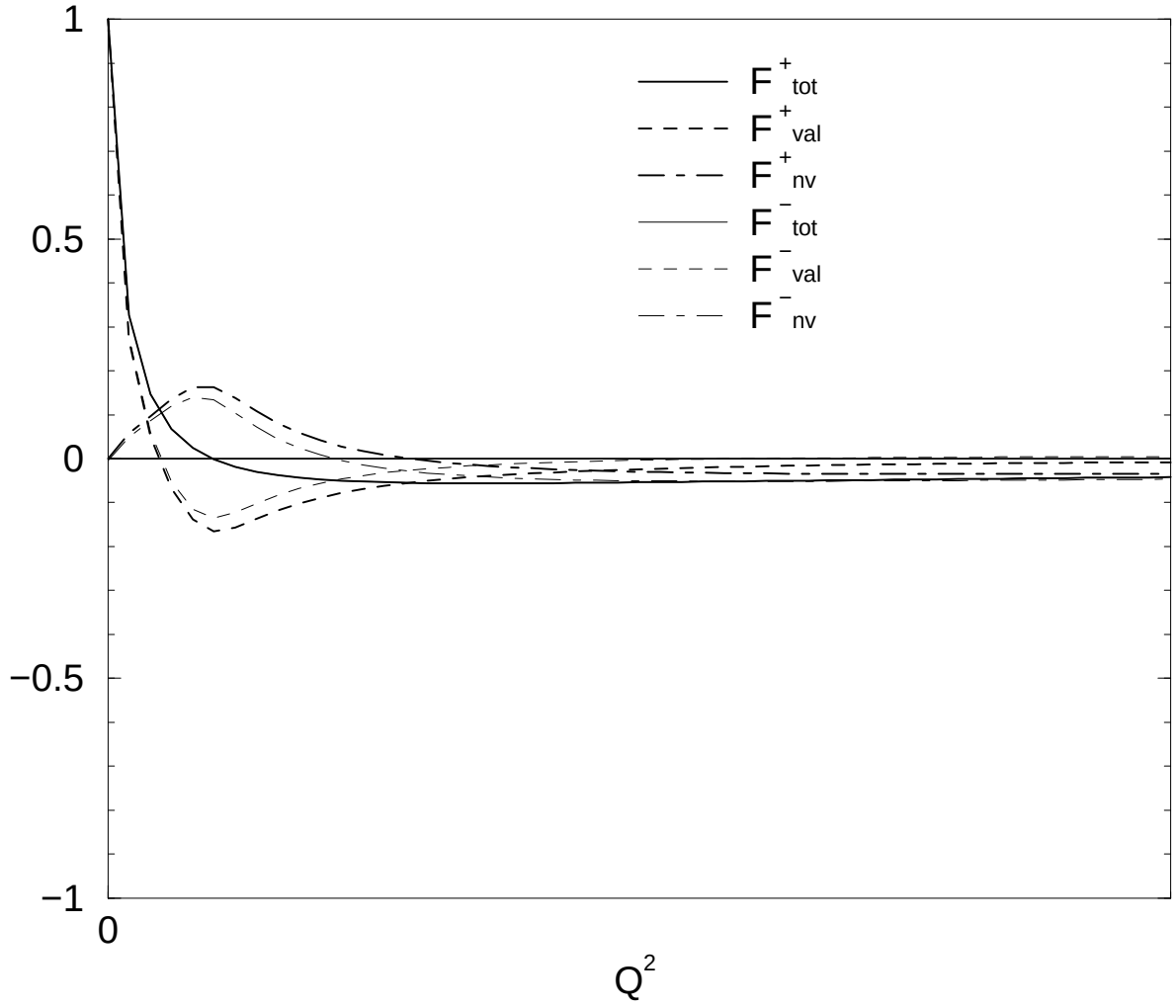

Mon Jan 31 15:20:36 2000